

# The morphogenesis of feathers

Mingke Yu, Ping Wu, Randall B. Widelitz & Cheng-Ming Chuong

Department of Pathology, Keck School of Medicine, University of Southern California, 2011 Zonal Avenue, Los Angeles, California 90033, USA

Feathers are highly ordered, hierarchical branched structures<sup>1,2</sup> that confer birds with the ability of flight<sup>3–5</sup>. Discoveries of fossilized dinosaurs in China bearing ‘feather-like’ structures have prompted interest in the origin and evolution of feathers<sup>6–14</sup>. However, there is uncertainty about whether the irregularly branched integumentary fibres on dinosaurs such as *Sinornithosaurus* are truly feathers<sup>11</sup>, and whether an integumentary appendage with a major central shaft and notched edges is a non-avian feather or a proto-feather<sup>8–10</sup>. Here, we use a developmental approach to analyse molecular mechanisms in feather-branching morphogenesis. We have used the replication-competent avian sarcoma retrovirus<sup>15</sup> to deliver exogenous genes to regenerating flight feather follicles of chickens. We show that the antagonistic balance between noggin and bone morphogenetic protein 4 (BMP4) has a critical role in feather branching, with BMP4 promoting rachis formation and barb fusion, and noggin enhancing rachis and barb branching. Furthermore, we show that sonic hedgehog (Shh) is essential for inducing apoptosis of the marginal plate epithelia, which results in spaces between barbs. Our analyses identify the molecular pathways underlying the topological transformation of feathers from cylindrical epithelia to the hierarchical branched structures, and provide insights on the possible developmental mechanisms in the evolution of feather forms.

With three levels of branching (that is, from rachis to barbs; from

barbs to barbules; and from barbules to cilia or hooklets<sup>1</sup>; Fig. 1a) feathers can develop into a variety of forms, including downy feathers, contour feathers, or flight feathers (Fig. 1b). As in hairs, the feather follicle is composed of a dermal papilla and epidermal collar (equivalent to the hair matrix, Fig. 1c–f). Through epithelial–mesenchymal interactions, the epithelial cells at the bottom of the follicle undergo active proliferation (proliferation zone, Fig. 1c). Immediately above this zone, the epithelial cells start to form the rachidial ridge and the barb ridges (ramogenic zone, Fig. 1c)<sup>16–19</sup>. In a more distal position along the follicle, the barb ridge epithelia actively proliferate and differentiate to form the marginal plates, barbule plates and axial plates (Fig. 1g). The barb ridges grow to form barbs, composed of the ramus and barbules, whereas the marginal and axial plate cells die to become the intervening space. Individual barbule plate cells undergo further cell shape changes to form the cilia and hooklets<sup>1</sup>. The barb ridges fuse proximally to form the rachidial ridge, which eventually becomes the rachis. Additional cross-sections (Supplementary Fig. 1) illustrate this process.

The cellular and molecular mechanisms of epithelial organ morphogenesis are beginning to be understood<sup>20,21</sup>. Although branching morphogenesis<sup>21</sup> has been studied in the lung and kidney, branching in the feather is unique owing to its exquisite order and non-randomness. Here, we studied the role of noggin–BMP interactions that underlie the fundamental morphogenetic mechanisms<sup>22–24</sup> in this process. We first analysed the dynamic expressions of BMP2, BMP4 and noggin in remiges (flight feathers) of 15-day-old chicken embryos (E15) using *in situ* hybridization. BMP4 transcripts were detected in the dermal papilla and overlying pulp area (Fig. 1d). At a later time point, BMP4 was expressed in barbule plate cells (Supplementary Fig. 2). BMP2 was present in the marginal plate epithelia in early ramogenesis<sup>25</sup>, but quickly switched to barbule plate epithelia (Fig. 1f, h, i). BMP4 expression in the

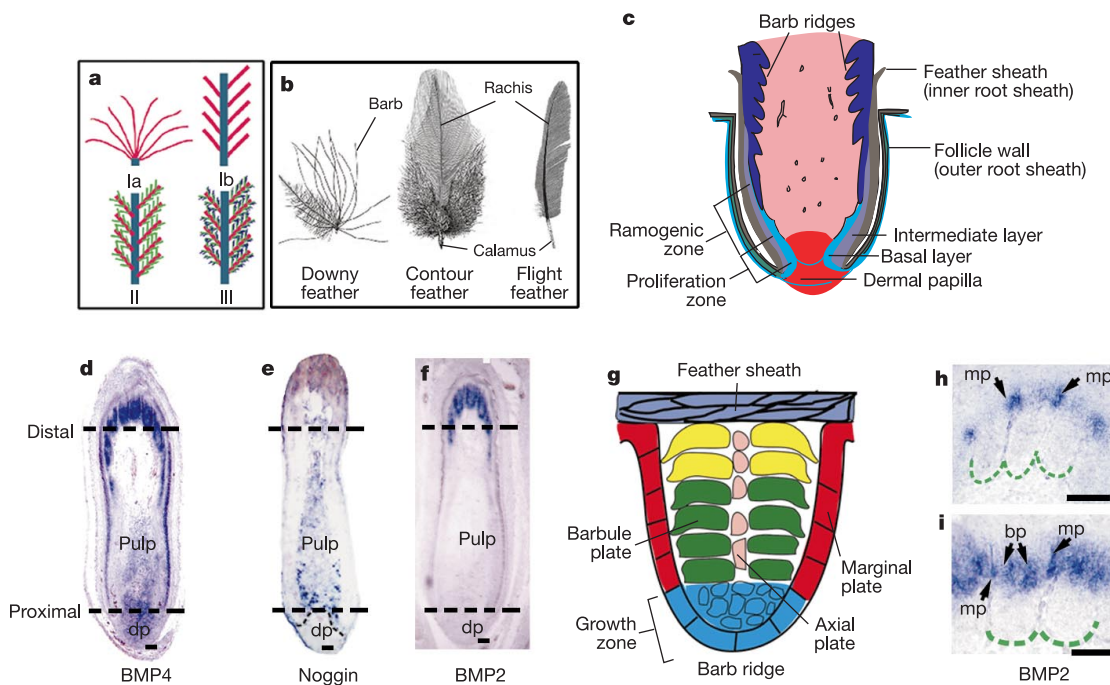


**Figure 1** Feather-branching morphogenesis and gene expression. **a**, Diagram showing three branching levels. Level I, rachis (blue) branches into barbs (red). Ia, radially and Ib, bilaterally symmetric feathers. Level II, barbs branch into barbules (green); level III, barbules branch into cilia and hooklets (purple). **b**, Different types of chicken feather. **c**, Diagram of feather follicle structure. **d–f**, BMP4 (**d**), noggin (**e**) and BMP2 (**f**) expression

patterns. The two dotted lines indicate the level of cross-sections shown in Supplementary Fig. 2. **g**, Diagram of feather barb ridge. **h, i**, BMP2 in barb ridges. BMP2 is expressed first in peripheral marginal plates (mp; **h**) then switches to barbule plates (bp; **i**). dp, dermal papilla. Scale bar, 100 μm.

mesenchyme appeared to form a gradient, tapering from the proximal to distal regions (Fig. 1d). Noggin transcripts were detected in the pulp cells, overlapping with BMP4 transcripts. Noggin was not expressed in the dermal papilla, but was expressed in the pulp regions adjacent to the epidermis. The expression level of noggin appeared to form a gradient from the proximal to distal pulp, with highest expression at the level of the ramogenic zone (Fig. 1e). Cross-sections at the indicated locations (dotted lines) are also shown (Supplementary Fig. 2).

A distinct feature of feathers is that they can regenerate repetitively after plucking. Remige feathers regenerate at a rate of about  $0.5 \text{ cm day}^{-1}$ , making them excellent recipients for replication-competent avian sarcoma retrovirus (RCAS)-mediated gene expression, which only transduces cells undergoing active mitosis<sup>15</sup>. By injecting RCAS retroviral constructs into chick flight feather follicles after plucking (Fig. 2a), exogenous genes were misexpressed during feather regeneration (Fig. 2b, Supplementary Fig. 3). Regenerated feathers injected with RCAS–LacZ virus showed no changes in the formation of rachis or barbs (Fig. 2c, g).

RCAS–noggin was injected into the feather follicles to perturb their BMP activity (Fig. 2d, h;  $n = 36$ ). Many of the regenerated feathers were severely stunted, forming few barbs (33%), and even more had the rachis split into two or four mini-rachides (44%). These smaller rachides gradually converged at the proximal end (Fig. 2d). Barbs of the regenerated feathers expressing exogenous noggin were inhibited (50%) and some barbs (11%) branched into two (Fig. 2h). Histological examination showed that the barb ridges formed irregular tree-like structures with extravagant ridge formations (Fig. 3b, f, j). The rachidial ridge was fragmented into smaller ridges (Fig. 3n).

Regenerated feathers expressing ectopic BMPs had phenotypes that were generally opposite to that of feathers expressing exogenous noggin. Many of the regenerated feathers transduced with

RCAS–BMP4 were short in length, did not form barbs or a rachis (50%), and assumed a morphology similar to the calamus (feather shaft) ( $n = 16$ ). Several of the rachides on these regenerated feathers were oversized (25%). Ectopic rachis-like structures were observed (Fig. 2e; 31%) and the barbs were often fused (Fig. 2i; 38%). Histological sections showed that the barb ridges failed to separate (Fig. 3c, g), the barbs fused (Fig. 3k) and the rachidial ridges were oversized (Fig. 3o). The presumptive marginal plate cells became plump (Fig. 3g) and did not die, thus preventing the creation of spaces between barbs (Fig. 3k).

Overexpression of BMP2 had similar phenotypic effects to BMP4. Feathers showed normal growth at first, but then died abruptly and fell off prematurely at about 3 weeks. The feather size was usually smaller and some showed no barb formation. The rachides of the regenerated feathers were enlarged (Fig. 2f; 23%,  $n = 26$ ) and some feathers had ectopic rachides (23%). Some barbs fused with each other or with the rachis at various points, forming bundles (Fig. 2f, j; 77%). Histological sections showed that some barb ridges fused in pairs (Fig. 3h), suggesting that BMP2 may also function in specifying marginal plate fate, given that BMP2 is expressed transiently in peripheral marginal plates (Fig. 1h). Ectopic rachidial ridge-like structures caused by the fusion of barb ridges were observed (Fig. 3l). The rachidial ridge was extremely large, spanning nearly half of the follicle circumference (Fig. 3p). Thus, the phenotypes of regenerated feathers appeared to depend on the expression levels of the transduced genes.

Whereas abnormal barb ridges shared a forked appearance, the identity of barb branching or barb fusion was confirmed by counting the number and spacing of barbs. Control samples had about six barb ridges in the space shown in Fig. 3e–h. Specimens treated with noggin had elaborately branched ridges alternating with mini-ridge forms, but the total number of ridges was unchanged. Specimens treated with BMP2 had only three forked barb ridges, suggesting that fusion occurred among the original six ridges.

Marginal plate cells express *Shh*<sup>26</sup> whereas barbule plate cells express feather keratin (Figs 3q, u and 4a). Characterization of the transduced feathers showed that noggin increased branching by increasing the number of *Shh*-positive marginal plate cells (Fig. 3r) and that it perturbed the shape and arrangement of the barbule plate cells that express feather keratin (Fig. 3v). On the other hand, epithelial overexpression of BMP2 and BMP4 altered the fate of marginal plate cells. The cells, which were plump rather than flattened (Fig. 3g, k) did not die, and branches failed to form. In addition, *Shh* was not expressed (Fig. 3s, t). Some feather keratinization still took place in the barbule plate (Fig. 3w, x).

To test further the role of *Shh* in feather branching, we suppressed *Shh* using cyclopamine<sup>27</sup> or RCAS–antisense *Shh* in the plucked and regenerating feather model. The two independent reagents gave similar results. The regenerated feathers showed regions where barbs were fused by means of a web-like membrane, thus forming continuous feather vanes (Fig. 4b, c). Cross-sections showed regions with barb ridges that failed to separate because the marginal plate cells failed to disappear (Fig. 4d, e). Suppressing *Shh* produced a similar phenotype as the overexpression of BMP4 (compare Figs 3g and 4e). In control feathers, TdT-mediated dUTP nick end labelling (TUNEL) staining was positive in the marginal epithelial cells, pulp epithelium and feather sheath (Fig. 4f). The death of these cells allows feather branches to open. Suppression of *Shh* activity increased the number of marginal plate cells. These cells were plump in appearance and were mostly TUNEL negative (Fig. 4g). Thus, overexpression of BMP suppressed *Shh* expression and the subsequent formation of the marginal plate. Suppression of BMP promoted branching, probably by enhancing ridge-forming activity of the basilar cells, together with specifying the fate of marginal plate cells. Therefore *Shh* is required for specification of the fate of marginal plate cells. Balancing the antagonistic actions of *Shh* and

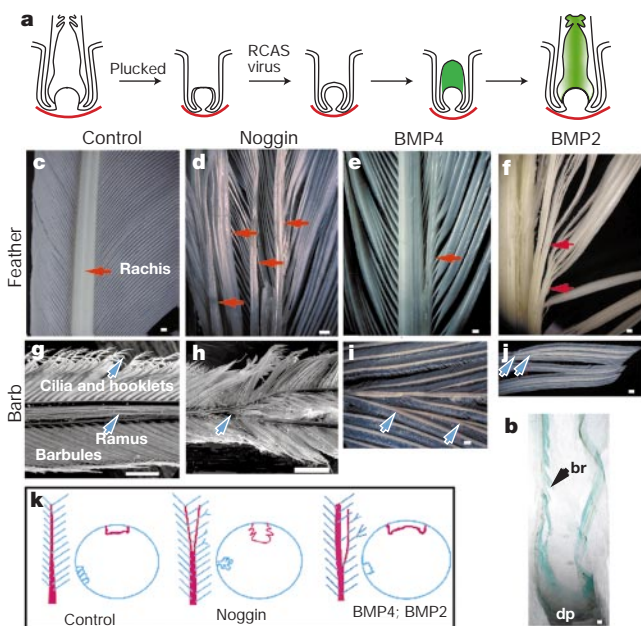


**Figure 2** Phenotypic changes in feathers regenerated from follicles injected with RCAS–noggin, RCAS–BMP4 and RCAS–BMP2, respectively. **a**, Diagram showing gene expression strategy. **b**, X-gal staining of a regenerating feather follicle 7 days after RCAS–LacZ injection. **c–f**, Splitting or merging of the rachis is indicated by red arrows. **g–j**, Alteration of the barbs. Abnormal branch points are indicated by blue arrows. **k**, Diagram illustrating the overall phenotypic changes. br, barb ridge; dp, dermal papilla. Scale bar: **b–f, i, j**, 200  $\mu\text{m}$ ; **g, h**, 100  $\mu\text{m}$ .

## letters to nature

BMPs sets the number and spacing of barb ridges; however, regulation of Shh by other molecules is also possible.

The importance of the Shh–BMP ‘signalling module’<sup>28</sup> in skin appendage morphogenesis has also been shown by comparing chicken feather variants, duck feathers, and avian and alligator scales<sup>25</sup>. Using embryonic chicken explant cultures, this study indicated that Shh is important for proliferation in proximal barb ridges, whereas BMP2 suppresses Shh and promotes differentiation of distal barb ridges<sup>25</sup>. Our *in vivo* ‘transgenic feather’ model using plucked/regenerated mature feather follicles allows us to analyse the late-branching event that is impossible to observe in embryonic explants. This model should make it possible for future experiments to link molecular pathways with feather forms.

On the basis of these data, we propose the following model for feather-branching morphogenesis (Fig. 5a, b). The multilayered epidermis can be moulded into epidermal ridges by ridge-forming activators (for example, noggin) and inhibitors (for example, BMPs) distributed in the adjacent mesenchyme. The balance between noggin and BMP4 determines the number, size and spacing of barb ridges. First, at the proliferation zone, the level of BMP4 is much higher than that of noggin, thus the epithelial cells form a cylindrical structure. Second, at the ramogenic zone, the level of

noggin in the pulp adjacent to epithelia gradually exceeds that of BMP4, thus the epithelial cells start to form multiple barb ridges. Third, the basilar layer becomes periodically arranged into Shh positive/BMP2 transiently positive marginal plate cells that die and Shh negative cells from the barb ridge growth zone that proliferate. The intermediate cell layer is ‘cleaved’ into groups of cells that become the initial barb ridge. Marginal plate cells die to ensure the formation of spaces between barb ridges<sup>1,29</sup>. Fourth, the originally randomly arranged cells in the barb ridge express BMP2 and BMP4, line up, and become two rows of barbule cells. These cells further differentiate to form the barbules. Barbule plate cells<sup>1</sup> stimulated by BMP2 and BMP4 change shape to form the cilia and hooklets. Fifth, towards the end of feather formation, noggin activity is reduced and conditions revert back to stage one, forming the calamus without branches at the proximal end of the feather shaft. Last, if the noggin:BMP ratio becomes polarized in the anterior–posterior axis, the site with higher BMP activity eventually becomes the rachis, thus the bilaterally symmetric feather can form.

We have demonstrated that the BMP pathway regulates the formation and inter-conversion of the barbs and rachis. We have also shown that the true separation of branches requires Shh activity. Other morphogens, such as fibroblast growth factors

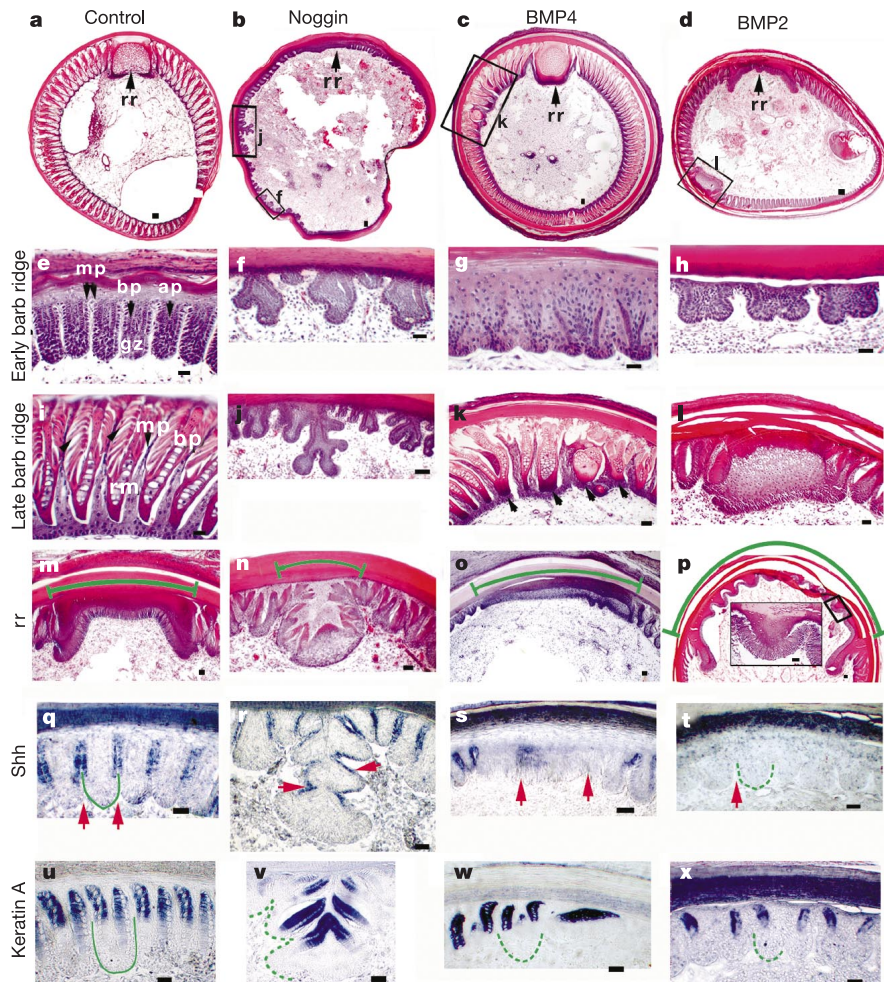


**Figure 3** Analyses of feathers injected with RCAS–noggin, RCAS–BMP4 and RCAS–BMP2, respectively. **a–d**, Cross-sections of a feather. **e–l**, Changes in barb ridges. **m–p**, Changes of rachis width (stained with haematoxylin and eosin). The rachis width is indicated by a green arc. The inset in **p** is part of the rachis structure, not barb ridges (compare with **e**). **q–t**, *In situ* hybridization with Shh probes. Marginal plates or

comparable regions are indicated with red arrows. **u–x**, *In situ* hybridization with feather keratin probes. Green lines delineate barb ridges; dotted lines indicate abnormal barb ridges. ap, axial plate; bp, barbule plate; gz, barb ridge growth zone; mp, marginal plate; rr, rachis ridge. Scale bar, 100  $\mu$ m.

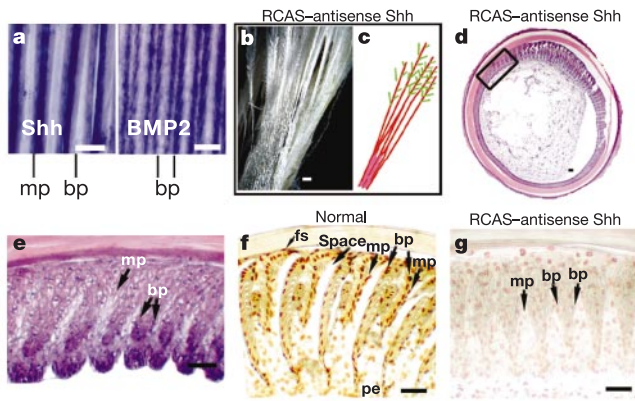


**Figure 4** The role of Shh in barb formation. **a**, Normal feather whole-mount *in situ* hybridization of Shh and BMP2. **b**, Shh inhibition by RCAS-antisense Shh or cyclopamine produces fused vanes. **c**, Diagram showing changes in **b**. Barbs are red and barbules are green. **d**, Cross-sections (stained with haematoxylin and eosin) show barb ridge segments that fail to separate, varying from more severe (bottom left quarter of cross-section) to less severe (top right segment). **e**, Greater magnification of boxed section in **d**. **f, g**, Apoptosis in late-differentiated barb ridges in normal and Shh-suppressed follicles. bp, barbule plate; fs, feather sheath; mp, marginal plate; pe, pulp epithelium. Scale bar, 100  $\mu$ m.

(FGFs) and Wnts<sup>18</sup>, may also be involved in this process, and we expect them to behave under similar principles along the same pathway or with special regulation to produce feather variants.

Formation of hierarchical branches is the principal feature of feathers<sup>17</sup>, and is therefore one of the chief issues in the origin and evolution of feathers. On the basis of some fossil evidence it has been proposed that a filamentous integument structure with a major central shaft and notched edges may be the prototype of feathers<sup>8-10</sup>. According to this model, the rachis would have formed first in evolution, then barbs, and finally barbules. Therefore, the rachis and barbs would be different entities and not interchangeable (Fig. 5c). Alternatively, because barbs form first during development, it was proposed that barbs appeared first in integument evolution, and the rachis, a specialized form of fused barbs, appeared later as an evolutionary novelty<sup>16,18</sup>. The fact that the barbs and the rachis

can be converted experimentally in the laboratory favours the barb to rachis model. Our data suggest that a radially symmetric feather is more primitive than the bilaterally symmetric feather in terms of molecular and developmental mechanisms, and may have been the prototype of feathers (Fig. 5c). Some fossilized primitive skin appendages on *Sinornithosaurus* also favour this model<sup>11</sup>. Further modulation of BMP and Shh pathways may have led to the many varieties of feather seen today by regulating the number, shape and size of the rachis, barbs, and barbules<sup>1,17,30</sup>. This work provides evidence for the molecular mechanisms possibly involved in the evolution of feather branching. □

**Methods**

**Materials**

Specific pathogen-free, fertilized white leghorn chicken eggs were purchased from Charles River SPAFAS. The eggs were incubated at 38 °C in a humidified rotating incubator. Chicks were housed in the University of Southern California vivarium. Digoxigenin-labelled probes were generated by *in vitro* transcription from plasmids provided by L. Niswander for noggin, P. Francis-West for BMP2 and BMP4, and C. Tabin for Shh. A probe for feather keratin was prepared in our laboratory, GenBank accession number X 17511. RCAS-noggin plasmid was from R. Johnson; RCAS-BMP2 and RCAS-BMP4 plasmids were from P. Francis-West; RCAS-LacZ plasmid encoding  $\beta$ -galactosidase was originally constructed by L. Yi and was provided by W.-P. Wang; RCAS-Shh sense was from C. Tabin; RCAS-Shh antisense was produced by cutting the sense Shh plasmid with *Clal* and re-ligating the inserted Shh in the reverse orientation. The orientation was confirmed by restriction enzyme analysis (S. A. Ting-Bereth and C.-M.C., unpublished data). Viruses were prepared and titrated<sup>24</sup>. Cyclopamine, a Shh antagonist<sup>26</sup> provided by W. Gaffield, was dissolved in absolute ethanol and diluted to 0.4 mg ml<sup>-1</sup> in DMEM for injection (20  $\mu$ l) into the regenerating feathers, using a similar procedure described for viral transduction.

**Transduction of regenerating feather follicles**

Chickens at 2-3 weeks of age were anaesthetized with ketamine (50 mg per kg body mass). Primary remiges I to VII were used because of their large size, distinct morphology and identity. Normally, feathers will regenerate and grow out of the follicles at about 14 days after plucking. Regenerated feathers/feather follicles were dissected at 7 days after plucking. Serial longitudinal and cross paraffin sections were cut and stained with haematoxylin and eosin. For gene transduction, RCAS viruses were injected into the empty follicles immediately after feathers were plucked. RCAS virus propagation in follicles was verified using RCAS-LacZ virus followed by 5-bromo-4-chloro-3-indolyl- $\beta$ -D-galactoside (X-gal) staining of cryostat sections at various days after the injection. Each follicle received about 10-20  $\mu$ l of medium containing the virus ( $1 \times 10^5$  to  $1 \times 10^6$  infectious units per ml). For preliminary studies, viruses containing the genes of interest were injected into primary remige follicles on the left wing. RCAS-LacZ virus was injected into primary remige follicles on the right wing as controls. Feather follicles injected with viruses were dissected and sectioned for histological study at 2-3 weeks after virus injection. Once distinct phenotypes were confirmed in at least three repeat experiments,

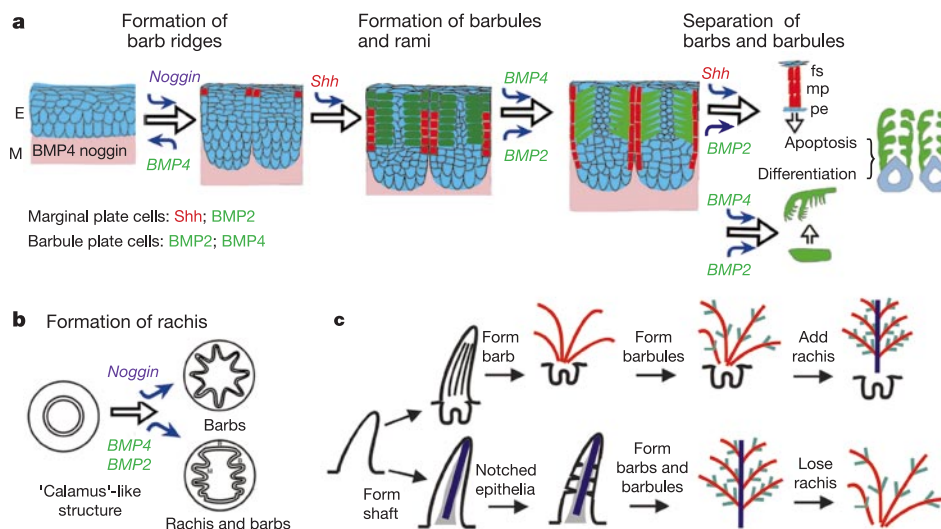


**Figure 5** Models of feather branching and evolution of feather forms. **a**, Roles of noggin/BMP4, Shh and BMP2 in the three levels of feather branching. E, epithelial cells (blue); M, mesenchymal cells (pink). fs, feather sheath; mp, marginal plate; pe, pulp epithelium. **b**, The ratio of noggin and BMP4 may determine the number and size of barb ridges. A

localized high BMP:noggin ratio, together with a helical growth mode of barb ridges<sup>17</sup>, can lead to the formation of a rachidial ridge through fusion of barb ridges. **c**, Hypothetical models of the evolution of feather forms. Top row, barb to rachis model; bottom row, rachis to barb model. The experimental data are in favour of the barb to rachis model.

viruses were injected to follicles on both wings for later studies. Chickens were raised in cages and observed on a daily basis over a two-month period. The regenerated feathers were plucked and examined with a dissection or scanning electron micrograph microscope for abnormalities compared with normal primary remiges.

## Histology and *in situ* hybridization

Paraffin sections (5 µm) were stained with haematoxylin and eosin or prepared for *in situ* hybridization following routine procedures<sup>26</sup>. Cryostat sections (10 µm) were stained with X-gal. TUNEL staining was performed using a kit (Roche). Nonradioactive wholemount or section *in situ* hybridization or section *in situ* hybridization was performed according to the protocol described<sup>22,26</sup>. After hybridization, sections were incubated with an anti-digoxigenin Fab conjugated to alkaline phosphatase (Boehringer Mannheim). Colour was detected by incubating with a Boehringer Mannheim purple substrate (Roche).

Received 5 June; accepted 10 October 2002; doi:10.1038/nature01196.  
Published online 30 October 2002.

- Lucas, A. M. & Stettenheim, P. R. (eds) *Avian Anatomy – Integument. Agricultural Handbook 362: Agricultural Research Services* (US Department of Agriculture, Washington DC, 1972).
- Chuong, C.-M. The making of a feather: Homeoproteins, retinoids and adhesion molecules. *BioEssays* **15**, 513–521 (1993).
- Feduccia, A. *The Origin and Evolution of Birds* 2nd edn (Yale Univ. Press, New Haven, Connecticut, 1999).
- Chatterjee, S. *The Rise of Birds* (John Hopkins Univ. Press, Baltimore, Maryland, 1997).
- Regal, P. J. The evolutionary origin of feathers. *Q. Rev. Biol.* **50**, 35–66 (1975).
- Chen, P. J., Dong, Z. M. & Shen, S. N. An exceptionally well-preserved theropod dinosaur from the Yixian Formation of China. *Nature* **391**, 147–152 (1998).
- Xu, X., Tang, Z. L. & Wang, X. L. A therizinosauroid dinosaur with integumentary structures from China. *Nature* **399**, 350–354 (1999).
- Jones, T. D. *et al.* Nonavian feathers in a late Triassic archosaur. *Science* **288**, 2202–2205 (2000).
- Prum, R. O. Longisquama fossil and feather morphology. *Science* **291**, 1899–1902 (2001).
- Zhang, F. & Zhou, Z. A primitive enantiornithine bird and the origin of feathers. *Science* **290**, 1955–1959 (2000).
- Xu, X., Zhou, Z. & Prum, R. O. Branched integumentary structures in Sinornithosaurus and the origin of feathers. *Nature* **410**, 200–204 (2001).
- Ji, Q., Currie, P. J., Norell, M. A. & Ji, S. A. Two feathered dinosaurs from northeast China. *Nature* **393**, 753–761 (1998).
- Ji, Q., Norell, M. A., Gao, K. Q., Ji, S. A. & Ren, D. The distribution of integumentary structures in a feathered dinosaur. *Nature* **410**, 1084–1088 (2001).
- Norell, M. *et al.* Modern feathers on a non-avian dinosaur. *Nature* **416**, 36–37 (2002).
- Morgan, B. A. & Fekete, D. M. Manipulating gene expression with replication-competent retroviruses. *Methods Cell Biol.* **51**, 185–218 (1996).
- Prum, R. O. Development and evolutionary origin of feathers. *J. Exp. Zool.* **285**, 291–306 (1999).
- Prum, R. O. & Williamson, S. Theory of the growth and evolution of feather shape. *J. Exp. Zool.* **291**, 30–57 (2001).
- Chuong, C.-M., Chodankar, R., Widelitz, R. B. & Jiang, T.-X. Evo-devo of feathers and scales: building complex epithelial appendages. *Curr. Opin. Genet. Dev.* **10**, 449–456 (2000).
- Chuong, C.-M. *et al.* Dinosaur's feather and Chicken's tooth? Tissue engineering of the integument. John Ebling lecture. *Eur. J. Dermatology* **11**, 286–292 (2001).
- Chuong, C.-M. (ed.) *Molecular Basis of Epithelial Appendage Morphogenesis* (Landes Bioscience, Austin, 1998).
- Hogan, B. L. M. Morphogenesis. *Cell* **96**, 225–233 (1999).
- Jung, H.-S. *et al.* Local inhibitory action of BMPs and their relationships with activators in feather formation: implications for periodic patterning. *Dev. Biol.* **196**, 11–23 (1998).
- Dudley, A. T. & Tabin, C. J. Constructive antagonism in limb development. *Curr. Opin. Genet. Dev.* **10**, 387–392 (2000).
- Jiang, T.-X., Jung, H.-S., Widelitz, R. B. & Chuong, C.-M. Self organization of periodic patterns by dissociated feather mesenchymal cells and the regulation of size, number and spacing of primordia. *Development* **126**, 4997–5009 (1999).
- Harris, M. P., Fallon, J. F. & Prum, R. O. Shh-Bmp2 signaling module and the evolutionary origin and diversification of feathers. *J. Exp. Zool.* **294**, 160–176 (2002).
- Ting-Berthel, S. A. & Chuong, C.-M. Sonic hedgehog in feather morphogenesis: induction of mesenchymal condensation and association with cell death. *Dev. Dyn.* **207**, 157–170 (1996).
- Cooper, M. K., Porter, J. A., Young, K. E. & Beachy, P. A. Teratogen-mediated inhibition of target tissue response to Shh signaling. *Science* **280**, 1603–1607 (1998).
- Calabretta, R., Nolfi, S., Parisi, D. & Wagner, G. P. Duplication of modules facilitates the evolution of functional specialization. *Artificial Life* **6**, 69–84 (2000).
- Chuong, C.-M. & Edelman, G. M. Expression of cell adhesion molecules in embryonic induction. II. Morphogenesis of adult feathers. *J. Cell Biol.* **101**, 1027–1043 (1985).
- Gill, F. B. *Ornithology*, 2nd edn (Freeman, New York, 1994).

**Supplementary Information** accompanies the paper on Nature's website  
(<http://www.nature.com/nature>).

**Acknowledgements** We thank M. Ramos for help in preparing the manuscript; and R. Prum for critical comments on the manuscript. Figure 1b is modified from ref. 1. This work is supported by grants from the National Institute of Arthritis and Musculoskeletal and Skin Diseases, USA, and the National Science Foundation to C.-M.C., and a National Cancer Institute grant to R.B.W.

**Competing interests statement** The authors declare that they have no competing financial interests.

**Correspondence** and requests for materials should be addressed to C.-M.C.  
(e-mail: [chuong@pathfinder.usc.edu](mailto:chuong@pathfinder.usc.edu)).

# The genome sequence and structure of rice chromosome 1

Takuji Sasaki\*, Takashi Matsumoto\*, Kimiko Yamamoto\*, Katsumi Sakata\*, Tomoya Baba\*, Yuichi Katayose\*, Jianzhong Wu\*, Yoshihito Niimura†, Zhukuan Cheng‡, Yoshiaki Nagamura\*, Baltazar A. Antonio\*, Hiroyuki Kanamori\*, Satomi Hosokawa\*, Masatoshi Masukawa\*, Koji Arikawa\*, Yoshino Chiden\*, Mika Hayashi\*, Masako Okamoto\*, Tsuyu Ando\*, Hiroyoshi Aoki\*, Kohei Arita\*, Masao Hamada\*, Chizuko Harada\*, Saori Hijishita\*, Mikiko Honda\*, Yoko Ichikawa\*, Atsuko Itonuma\*, Masumi Iijima\*, Michiko Ikeda\*, Maiko Ikeno\*, Sachie Ito\*, Tomoko Ito\*, Yuichi Ito\*, Yukiyo Ito\*, Aki Iwabuchi\*, Kozue Kamiya\*, Wataru Karasawa\*, Satoshi Katagiri\*, Ari Kikuta\*, Noriko Kobayashi\*, Izumi Kono\*, Kayo Machita\*, Tomoko Maehara\*, Hiroshi Mizuno\*, Tatsumi Mizubayashi\*, Yoshiyuki Mukai\*, Hideki Nagasaki\*, Marina Nakashima\*, Yuko Nakama\*, Yumi Nakamichi\*, Mari Nakamura\*, Nobukazu Namiki\*, Manami Negishi\*, Isamu Ohta\*, Nozomi Ono\*, Shoko Saji\*, Kumiko Sakai\*, Michie Shibata\*, Takanori Shimokawa\*, Ayahiko Shomura\*, Jianyu Song\*, Yuka Takazaki\*, Kimihiro Terasawa\*, Kumiko Tsuji\*, Kazunori Waki\*, Harumi Yamagata\*, Hiroko Yamane\*, Shoji Yoshiki\*, Rie Yoshihara\*, Kazuko Yukawa\*, Huisun Zhong\*, Hisakazu Iwama†, Toshinori Endo§, Hidetaka Ito§, Jang Ho Hahn||, Ho-Il Kim||, Moo-Young Eun||, Masahiro Yano\*, Jiming Jiang‡ & Takashi Gojobori†

\* Rice Genome Research Program, National Institute of Agrobiological Sciences, and Institute of the Society for Techno-innovation of Agriculture, Forestry and Fisheries, 1-2, Kannondai 2-chome, Tsukuba, Ibaraki 305-8602, Japan  
† Center for Information Biology and DNA Data Bank of Japan, National Institute of Genetics, Mishima 411-8540, Japan  
‡ Department of Horticulture, University of Wisconsin-Madison, Madison, Wisconsin 53706, USA  
§ Department of Bioinformatics, Tokyo Medical and Dental University, 1-5-45 Yushima, Bunkyo-ku, Tokyo 113-8510, Japan  
|| Rice Genome Sequencing Project, National Institute of Agricultural Science and Technology, RDA, 249 Seodun-dong, Suwon 441-707, Korea

The rice species *Oryza sativa* is considered to be a model plant because of its small genome size, extensive genetic map, relative ease of transformation and synteny with other cereal crops<sup>1–4</sup>. Here we report the essentially complete sequence of chromosome 1, the longest chromosome in the rice genome. We summarize characteristics of the chromosome structure and the biological insight gained from the sequence. The analysis of 43.3 megabases (Mb) of non-overlapping sequence reveals 6,756 protein coding genes, of which 3,161 show homology to proteins of *Arabidopsis thaliana*, another model plant. About 30% (2,073) of the genes have been functionally categorized. Rice chromosome 1 is (G + C)-rich, especially in its coding regions, and is characterized by several gene families that are dispersed or arranged in tandem repeats. Comparison with a draft sequence<sup>5</sup> indicates the importance of a high-quality finished sequence.

Rice has been studied extensively by molecular genetics and constitutes one of the best characterized crop plants with a fine genetic map of 3,267 markers (<http://rgp.dna.affrc.go.jp/public-data/geneticmap2000/index.html>)<sup>1</sup>, a yeast artificial chromosome (YAC) physical map with 80.8% coverage<sup>2</sup>, sequences for about 10,000 unique expressed sequence tags (ESTs)<sup>3</sup>, and a transcriptional map indicating the placement of 6,591 unique ESTs<sup>2</sup>. The Rice Genome Research Program (RGP) in Japan launched its rice genome sequencing project in 1998. It is a partner of the International Rice Genome Sequencing Project (IRGSP), which involves ten countries in Asia, North America, South America and Europe that are working towards the immediate release of high-quality sequence data to the public domain<sup>4</sup>. The draft sequences of the two